Novel Active Contour Model-based Automated Segmentation of PET Images

Mingzan Zhuang, Rudi A. J. O. Dierckx, and Habib Zaidi, *Senior Member, IEEE*

***Abstract*— Although positron emission tomography (PET) has been commonly used in oncology, for radiation therapy treatment planning or the assessment of response to treatment, in view of the fact that the rate of glucose metabolism is increased in malignant tumours, it is not easily to delineate the boundaries of tumours from the surrounding normal tissue because of the low spatial resolution and inherent noisy characteristics in PET images. In this work, a novel method for automatic segmentation using an active contour model is presented. The algorithm incorporates histogram fuzzy C-means clustering and localized and textural information to constrain the active contour to detect boundaries in an accurate and robust manner. Moreover, the lattice Boltzmann method is used as an alternative approach for solving the level set equation to make it faster and suitable for parallel programming. The proposed method was compared with the contourlet-based active contour algorithm and Schaefer's thresholding method using phantom and clinical studies. Our results demonstrate that the developed novel PET segmentation algorithm is applicable to various types of lesions and is capable of producing accurate and consistent target volume delineations, potentially resulting in reduced intra- and inter-observer variability commonly observed when using manual delineation.**

***Index Terms*—PET imaging segmentation, active contour model**

I. Introduction

2-Deoxy-2-[^{18}F]fluoro-D-glucose (^{18}F-FDG) positron emission tomography (PET) imaging is of great importance for the diagnosis, staging, therapy monitoring, and prognosis and detection of recurrences or metastatic disease. The detailed information characterizing carcinoma metabolism in PET imaging, such as metabolically active tumour volume, is helpful in delineating the target tumour required for assessment of response to treatment or radiation therapy treatment planning. However, the low spatial resolution and inherent noisy characteristics of PET images make the delineation of the target volume much challenging, although there is already quite a large number of PET segmentation algorithms developed during the last few years. An open issue associated with the different methods for segmentation of target tumour concerns their variability and dependence on different images. Proposed approaches to delineate MATV in PET imaging include thresholding techniques, variational approaches, learning methods, and stochastic modeling-based methods. Recent reviews of state-of-the-art PET image segmentation techniques indicate that there is no optimal solution for all types of clinical oncology indications with respect to accuracy, precision, and efficiency [1]-[3]. In this work, we focus on combining existing algorithms into a novel region-based Method for Automatic Segmentation using an Active Contour model (MASAC) to enhance robustness and generalness rather than proposing yet another PET segmentation method. This algorithm incorporates both histogram fuzzy C-means (FCM) clustering and textural information to constrain the active contour to detect the boundaries in an accurate and robust way, without requiring the setting of user-defined parameters. Moreover, we make the algorithm more efficient and appropriate for parallel programming by taking the lattice Boltzmann method (LBM) as an alternative approach to solve the level set equation. The proposed model is quite general and can be applied in many clinical scenarios.

Mingzan Zhuang, Rudi A. J. O. Dierckx and Habib Zaidi are with the Department of Nuclear Medicine and Molecular Imaging, University of Groningen, The Netherlands. H. Zaidi is also with the Department of Nuclear Medicine and Molecular Imaging, Geneva University Hospital, Switzerland.

II. Methods

To overcome the problems caused by noisy characteristics and enhance reliability and robustness, we applied three transformed images to replace the original PET images to serve as inputs to the energy functional. The proposed method can be divided into three main parts: initially, we apply histogram FCM clustering, bilateral filter and Gabor transformation to PET images, respectively. All these three transformed images were used as inputs for the energy functional. Then, Otsu's thresholding method, selecting from the gray level histogram the threshold to minimize the intraclass variance of the pixels, was used for the initial contour in the active contour model. Finally, the evolution equation of LBM is used to solve the level set equation.

To evaluate the proposed method's performance, the proposed technique was evaluated using a range of simulated phantom and clinical data, including the ground truth contours corresponding to the "best estimate" from simulation template and macroscopic specimen. Phantom studies were performed using the 4D extended cardio-torso (XCAT) phantom, a realistic whole-body computer model based on nonuniform rational B-spline surfaces representing the human anatomy and physiology [4]. Realistic lesion shapes with three different levels of tracer uptake, to simulate the heterogeneities within the tumour, were modelled based on clinical PET images and incorporated within the XCAT phantom according to the procedures proposed by Le Maitre et al. [5]. The thresholding method was adopted in our study, to delineate different irregularly shaped heterogeneities within clinical tumours, and the 3D mesh of segmented contours was reconstructed using Amide software (FEI, USA) and converted into nonuniform rational B-spline (NURBS) surfaces with Rhinoceros software (CADLINK, France). To model tumors with heterogeneities more realistically, three different NURBS surfaces, each representing a specific activity level, were created. Finally, for PET simulation, the sinograms were generated using an

978-1-5090-1642-6/16/$31.00 ©2016 IEEE

analytical forward projector, and reconstructed by an Ordered Subsets Expectation Maximization (OSEM) algorithm implemented in the Software for Tomographic Image Reconstruction (STIR) modeling for a GE Discovery RX PET/CT scanner [6]. The attenuation maps generated at 511 keV were used for attenuation correction during image reconstruction. Ten different lesions were simulated in two different lung locations, without or with high activity in the nearby myocardium (volume range 3.26cm^3 - 41.44cm^3). The clinical studies include 6 cases of pharyngolaryngeal squamous cell carcinoma (PH, volume range 4.03cm^3 - 32.92cm^3) and 10 cases of non-small cell lung cancer (LU, volume range 1.12cm^3 - 46.28cm^3), where 3D contours of the ground truth were derived from the macroscopic specimen obtained after surgery.

To verify the performance of different techniques, this proposed method was also compared with the contourlet-based active contour algorithm (CAC) [7] and Schaefer's thresholding method (ST) [8]. Widely adopted image analysis metrics including the relative volume error (RE), Dice similarity coefficient (DSC) and classification error (CE) were used to evaluate quantitatively the results.

III. Results

For the simulated XCAT phantom studies (PS), MASAC and CAC provide similar segmentations of the different lesions, while ST fails to achieve reliable results. For MASAC, it can be observed that there is no major difference between the mean values of the metrics between phantom studies without high nearby activity (PS1) and phantom studies with nearby high background activity (PS2), indicating the robustness of MASAC in different clinical scenarios (Fig, 1). Figure 2 shows representative contours on realistic anthropomorphic phantom studies nearby high background activity. Figure 3 shows box-and-whisker plots for all metrics across the clinical studies. In 13 of the 14 patients involved in the study protocol with those presenting with connected high-uptake regions excluded (CS), the DSC for MASAC was found to be larger than 0.60 (mean 0.71), indicating a good quality of segmentation of the clinical studies. The contours extracted by the MASAC algorithm of a representative patient from the lung cancer studies are presented in Figure 4. It can be seen that the MASAC algorithm still performs well in the case of heterogeneous tumours with necrotic regions. The contours extracted by MASAC fit well the ground truth defined on the macroscopic specimen.

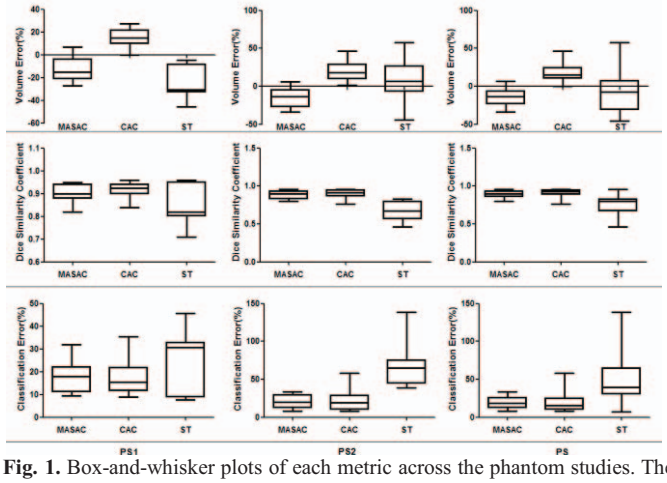

Fig. 1. Box-and-whisker plots of each metric across the phantom studies. The presented results represent phantom studies without nearby high activity (PS1), phantom studies with nearby high activity (PS2), and all phantom studies (PS).

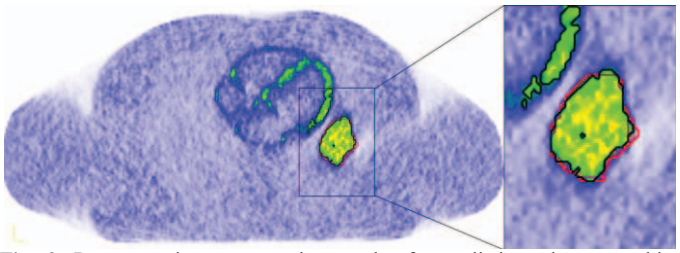

Fig. 2. Representative segmentation result of a realistic anthropomorphic phantom study (with nearby high activity in the myocardium) showing contours extracted by MASAC (purple), CAC (red) and ST (black), compared to the ground truth (orange). The initial cropping area has been shown on the rectangle area.

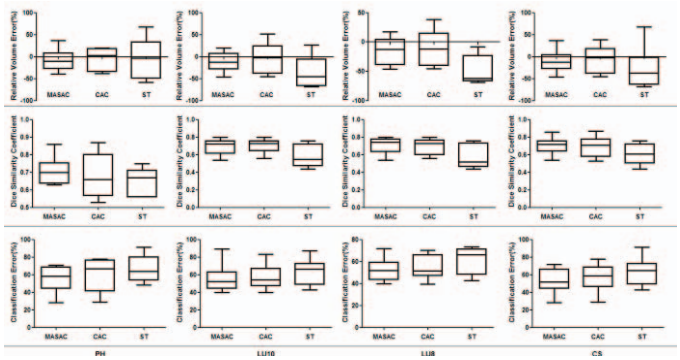

Fig. 3. Box-and-whisker plots of each metric across the clinical studies. The presented results represent 6 Louvain pharyngolaryngeal carcinoma studies (PH), 10 Louvain lung cancer studies (LU10), Louvain lung cancer studies with 2 studies presenting with connected high-uptake regions excluded (LU8), all clinical studies with 2 studies presenting with connected high-uptake regions excluded (CS).

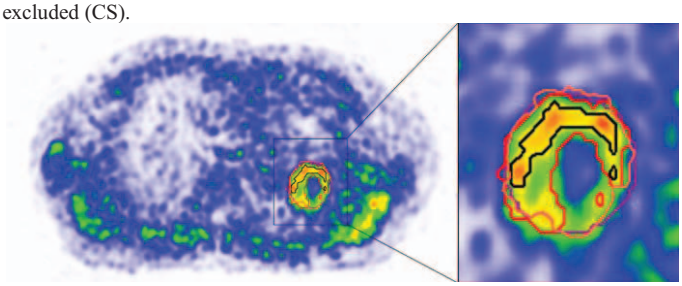

Fig. 4. Representative clinical non-small cell lung cancer PET study showing contours extracted by MASAC (purple), CAC (red) and ST (black), compared to the ground truth (orange). The initial cropping area has been shown on the rectangle area.

IV. Discussion - Conclusion

PET images provide information that can be used for application such as radiation therapy planning, therapy monitoring, patient prognosis and the detection of recurrences or metastatic disease. For these purposes, accurate delineation of the metabolic tumor volume in PET is of primary importance. Currently, there is still no commonly adopted technique for reliable routine clinical PET image auto-segmentation. In the presented work, we implement a generalized active contour model for PET image segmentation without prior knowledge, and extensively evaluate its performance with phantom and clinical data. The results have demonstrated its both feasibility

as well as ability to handle appropriately the intrinsic high noise level of PET images and the heterogeneity of the tumor uptake by incorporating histogram fuzzy C-means clustering and localized and textural information.

It can be noted that the MASAC algorithm has shown comparable or even better performance compared with those observed in other studies involving validation against clinical datasets. Our results using the PH database (6 studies) showed a mean DSC of 0.71 and mean CE of 55.64% compared with 0.54 and 50.20%, respectively, (for 7 studies) reported for a previous algorithm reported in our previous work [9]. The clinical assessment of the LU database (10 studies) resulted in mean DSC of 0.70 and mean CE of 56.21%, compared with 0.41 and 112.86% [9] and 0.54 and 60.58% [7] (9 studies), respectively. Schaefer et al. [10] evaluated consensus contours from different PET segmentation algorithms using clinical PET images and reported a mean DSC varying from 0.59 to 0.67.

Our results show that the application of histogram, localized, and textural features endows the MASAC algorithm with an extensive capture range, exhibiting robustness to various types of lesions assessed in our work, potentially resulting in reduced inter-observer variability of manual delineation and improved accuracy in treatment planning and outcome evaluation. Moreover, in order to enhance efficiency, we also employ the parallel programming to efficiently delineate structures boundaries. In this fast framework, we achieved execution times of 1 to 5 s for most of the cases, which could meet the daily clinical requirements. A number of techniques linked to this work have been reported in the literature. For instance, minimization of a joint energy derived from the sum of edge-based energies and region-based energies was suggested [11]. Lankton et al. [12] and Li et al. [13] provide the ways for localizing active contour models, using the convolutions with a specified mask function. Balla-Arabe et al. [14] focus on fast implementations employing the LBM that can be used to compute quickly and, hence, yield results in a much more efficient manner.

There are several practical limitations of this study [15]. First, the long examination duration of PET imaging might involve patient movement and motion artifacts. This aspect might further stimulate the research of 4D reconstruction. Second, the lesion less than 1 cm^3 is difficult to get a proper segmentation result. Further experience and research will also be needed to identify if high-resolution PET imaging is available. Another point to emphasize is that all the segmentation results were obtained from image characteristics. That means, provided an accurate image acquisition is used, this proposed method is likely to produce accurate segmentation for target volumes. Otherwise, it would be difficult to get the proper result. Moreover, we note that the cases in this study may not be sufficient, and our analysis is intended only as an initial examination for different segmentation methods. Further investigations are required to confirm our findings. Finally, in our PET simulation, we do not take the efficiency differences of the PET detectors into consideration. The assumption was also made that all images have the same constant random background to make the simulation less complex. Such procedures may also introduce some influence on the simulated images.

ACKNOWLEDGMENT

This work was supported by the Swiss National Science Foundation under Grant No. SNSF 31003A-149957, an Open Grant (No. 2014GDDSIPL-06) from the Key Laboratory of Digital Signal and Image Processing of Guangdong Province, Shantou University, and Shantou Medical Science Technology Project [No. (2014)62]. The authors would like to thank Dr. John Lee (Université Catholique de Louvain, Brussels) for providing the clinical PET datasets and Nicolas A. Karakatsanis and Zemian Chen for their assistance.

REFERENCES

[1] H. Zaidi and I. E. Naqa, "PET-guided delineation of radiation therapy treatment volumes: A survey of image segmentation techniques," Eur. J. Nucl. Med. Mol. Imaging, vol. 37, pp. 2165–2187, 2010.

[2] B. Foster, U. Bagci, A. Mansoor, Z. Xu, and D. J. Mollura, "A review on segmentation of positron emission tomography images," Comput. Biol. Med., vol. 50, pp. 76-96, 2014.

[3] J. A. Lee, "Segmentation of positron emission tomography images: Some recommendations for target delineation in radiation oncology," Radiother. Oncol., vol. 96, no. 3, pp. 302-307, 2010.

[4] W. P. Segars, G. Sturgeon, S.Mendonca, J. Grimes, and B.M.W. Tsui, "4D XCAT phantom for multimodality imaging research," Med. Phys., vol. 37, no. 9, pp. 4902-4915, 2010.

[5] A. Le Maitre, W. P. Segars, S. Marache, A. Reilhac, M. Hatt, S. Tomei, C. Lartizien, and D. Visvikis, "Incorporating patient-specific variability in the simulation of realistic whole-body F-18-FDG distributions for oncology applications," Proc. IEEE, vol. 97, no. 12, pp. 2026-2038, 2010.

[6] K. Thielemans, C. Tsoumpas, S. Mustafovic, T. Beisel, P. Aguiar, N. Dikaios, and M. W. Jacobson, "STIR: Software for tomographic image reconstruction release 2," Phys. Med. Biol., vol. 57, no. 4, pp. 867–883, 2012.

[7] M. Abdoli, R. A. J. O. Dierckx, and H. Zaidi, "Contourlet-based active contour model for PET image segmentation," Med. Phys., vol. 40, no. 8, pp. 082507, 2013.

[8] A. Schaefer, S. Kremp, D. Hellwig, C. Rübe, C. M. Kirsch, and U. Nestle, "A contrast-oriented algorithm for FDG-PET-based delineation of tumour volumes for the radiotherapy of lung cancer: Derivation from phantom measurements and validation in patient data," Eur. J. Nucl. Med. Mol. Imaging, vol. 35, no. 11, pp. 1989-1999, 2008.

[9] H. Zaidi, M. Abdoli, C. L. Fuentes, and I. M. E. Naqa, "Comparative methods for PET image segmentation in pharyngolaryngeal squamous cell carcinoma," Eur. J. Nucl. Med. Mol. Imaging, vol. 39, pp. 881-891, 2012.

[10] A. Schaefer, M. Vermandel, C. Baillet, A. S. Dewalle-Vignion, R. Modzelewski, P. Vera, L. Massoptier, C. Parcq, D. Gibon, T. Fechter, U. Nemer, I. Gardin, and U. Nestle, "Impact of consensus contours from multiple PET segmentation methods on the accuracy of functional volume delineation," Eur. J. Nucl. Med. Mol. Imaging, vol. 43, no. 5, pp. 911-924, 2016.

[11] N. Paragios, and R. Deriche, "Geodesic active regions: A new framework to deal with frame partition problems in computer vision," Int. J. Compus. Vis., vol. 46, no. 3, pp. 223-247, 2002.

[12] S. Lankton, and A. Tannenbaum, "Localizing region-based active contours," IEEE Trans. Image Process, vol. 17, no. 11, pp. 2029-2039, 2008.

[13] C. Li, C.Y. Kao, J. C. Gore, and Z. Ding, "Minimization of region-scalable fitting energy for image segmentation," IEEE Trans. Image Process, vol. 17, no. 10, pp. 1940-1949, 2008.

[14] S. Balla-Arabe, X. Gao, and B. Wang, "GPU accelerated edge-region based level set evolution constrained by 2D gray-scale histogram," IEEE Trans. Image Process, vol. 22, no. 7, pp. 2688-2698, 2013.

[15] M. Zhuang, R. A. Dierckx, and H. Zaidi, "Generic and robust method for automatic segmentation of PET images using an active contour model.," *Med Phys,* vol. 43, pp. 4483-4494, 2016.